Pergamon

Computerized Medical Imaging and Graphics, Vol. 20, No. 3, pp. 141–151, 1996

Printed in Great Britain
0895-6111/96 $15.00 + .00

PII: S0895-6111(96)00047-X

AN ATTEMPT TO 3D RECONSTRUCT VESSEL MORPHOLOGY FROM X-RAY PROJECTIONS AND INTRAVASCULAR ULTRASOUNDS MODELING AND FUSION

Claire Pellot,* Isabelle Bloch*† Alain Herment* and Francisco Sureda†
*INSERM U 66, CHU La Pitié Salpétrière, 91 Bd de l'Hôpital, 75013 Paris, France
†Ecole Nationale Supérieure des Télécommunications, Département Images, 46 rue Barrault, 75634 Paris, Cedex 13, France

(*Received* 31 *January* 1996; *accepted* 3 *June* 1996)

Abstract—The emergency of interventional revascularization techniques in the treatment of atheromateous vascular diseases has resulted in the need for additional valuable diagnostic information about the 3D morphology and nature of the lesion. To overcome the limitations inherent to common vascular imaging techniques, such as Digital Angiography (DA) which only gives partial information on lumen narrowing or Intravascular Ultrasound (IVUS) which provides randomly oriented transversal images, a 3D reconstruction of the vessel by fusion of X-ray and IVUS images has been developed.

For that purpose, X-ray and IVUS images are acquired according to a well-defined protocol and useful information to be fused is extracted. A geometric model then leads to the determination of the unknown parameters which allow the alignment of all data in a common reference frame. The registered data are then directly introduced into a probabilistic reconstruction process using a Markovian modeling associated with a simulated annealing-based optimization algorithm. Taking into account all the information available about the vessel, the method avoids the uncertainties and ambiguities of a reconstruction based only on one modality, and the probabilistic fusion solves the possible contradictions between both acquisitions.

Results of vascular lumen 3D reconstruction are shown with data acquired on an excised dog aorta. The accuracy of reconstruction of the lumen by data fusion is significantly improved compared to results obtained with separate reconstruction from angiographic or ultrasonic data. Further work will include introduction of vessel wall texture elements into the probabilistic fusion process to increase the amount of information gained by intravascular ultrasonic tissue characterization. Copyright © 1996 Elsevier Science Ltd.

Key Words: Vessel morphology, Medical imaging, Data fusion, 3D reconstruction, Digital angiography, Intravascular ultrasound, Geometric registration, Markovian modeling

INTRODUCTION

Atherosclerosis is the leading cause of mortality in industrial countries. The clinical manifestations of atherosclerosis include myocardial infarction, cerebrovascular stroke, and peripheral vascular disease.

Currently, vascular disease is best depicted with X-ray Digital Angiography (DA). DA provides detailed maps of the arterial lumen, in which atherosclerotic lesions are identified as local narrowings. Since lesions are not imaged directly but rather are inferred from luminal variations, angiographic techniques have several limitations. The severity of a stenosis may be underestimated if it is not seen from the optimal angle (lesions may be eccentric and have irregular shapes) or if the adjacent arteries are damaged.

A way to overcome that problem is to 3D reconstruct the vessel from different views. However, only a low number of views (usually two) can be acquired during an angiographic examination, since a reinjection of contrast medium between each acquisition is necessary and the quantity of contrast that the patient can tolerate is limited. As is well known, reconstruction from two projections is an ill-posed problem since there are many possible configurations having the same two projections. In a previous paper, we reported a method where the ill-posed nature of bi-planar reconstruction was regularized by incorporating anatomical *a priori* information through a Markov Random Field model (1). Although this method permits an efficient reconstruction with a close description of contour defects on simulated vessels and branchings, the quality of reconstruction on real angiograms is greatly damaged by uncertainties and inaccuracies on acquired data, both geometric due to the contribution of overlying structures and densitometric due to the inhomogeneous opacification of blood in DA procedures. Moreover, arteries are known to enlarge

in response to the development of an atherosclerotic plaque and luminal narrowing may not be evident until the plaque occupies more than 40% of the true luminal diameter (2). Thus, while DA is excellent for determining the site of a constriction, it provides little information about the atherosclerotic lesion or the arterial wall.

Additional diagnostic information about the nature of the lesion is required to maximize the effectiveness of catheter-based interventional procedures, such as percutaneous transluminal angioplasty (PTA) which dilates the artery by means of balloon inflation, or atherectomy, which removes arterial material from the site of a constriction. Indeed, PTA has a relatively high rate of restenosis (3) and is known to perform poorly in tortuous, constricted or calcified arteries, while atherectomy is known to damage the medial layer of the artery. A lower restenosis rate could be achieved if the material to be excised was identified more clearly.

Several modalities including Angioscopy and Intravascular Ultrasound (IVUS) have been developed to obtain information about vascular structure and disease, and assist the clinician in the classification of stenotic lesions and in the determination of the appropriate therapy (4, 5). IVUS provides high-resolution cross-sectional images of the lumen, arterial wall and adjacent tissue, thanks to a high-frequency catheter-mounted miniature transducer. It has the potential to define early-stage plaque and undulations or thickenings of the intima which denote plaque deposition or other pathology. However, considering that vessels and plaques are complex 3D structures and 2D images are acquired, a 3D reconstruction is required in order to depict these structures and accurately estimate plaque severity. Several methods for 3D reconstruction of vessels from intravascular tomographic slices have been proposed. Most of them consist of stacking and interpolating IVUS images, assuming a regular motion of the ultrasonic transducer (6). Other approaches consist of controlling the position of the catheter by a motorized system and stacking the ultrasonic slices according to the vessel curvature obtained from angiograms (7). However, given that the transducer freely moves inside the arterial lumen, the catheter trajectory is rarely coaxial with the vessel axis. In fact, reconstruction from IVUS data is greatly affected by physical acquisition factors—in particular uncertainties on the catheter position and orientation (8, 9).

To overcome these limitations, we propose a multi-modality fusion approach, that combines IVUS images first with X-ray non-opacified control projections which help in determining the relative positions and orientations of ultrasonic slices, and second with two post-contrast-injection X-ray angiographies. Indeed, these two modalities are well complementary and suitable for fusion since DA provides longitudinal projections of the vessel lumen while IVUS provides transversal cross-sections of the lumen and wall. The fusion here not only intends to match the two modalities but to really combine the different data, in order to provide a more complete description of the 3D vessel morphology and composition, and thus increase diagnostic information before and possibly during an intervention.

The feasibility of the multi-data fusion approach has been tested on an excised dog aorta, and the whole methodology has been applied to a representative segment of the aorta.

The paper is organized as follow: section 2 describes the acquisition protocol for X-ray and ultrasonic images. Section 3 describes the registration of IVUS slices and X-ray projections and the obtaining of an approximate ultrasonic volume, by means of a geometrical fusion. Section 4 describes the probabilistic fusion which consists of improving the geometric fusion by directly introducing the registered IVUS and DA data into a common Markovian model of the vessel. Finally, results obtained *in vitro* on the dog aorta are shown and discussed in section 5.

DATA OBTAINING

Material

For this feasibility test, *in vitro* images were acquired in conditions as close as possible to clinical examination, by using an animal artery sample, whose geometry as well as tissue echogenicity and X-ray attenuation are comparable to those of human arteries. The IVUS examination was manually driven since it is the case in clinical routine.

A dog aorta was excised during a cardiac mapping study and immersed in a solution of formol. It was subsequently made solid while maintaining its original shape with an epoxy resin, which also filled in the small arterial branchings. Tubes were connected at each extremity of the aorta, and the set was placed over three non-aligned metallic rings mounted in a Plexiglas container to respect the initial vessel curvature. The tubes went out of the container through two holes. The container was filled with water.

X-ray imaging was performed with a Polytron DA system (Siemens). A 170 mm field of view (FOV)

and 1024×1024 image matrix were used (pixel size about 0.15 mm).

IVUS images were acquired with a Hewlett-Packard IVUS system, with a 15 mm FOV and 456×456 matrix (pixel size about 0.03 mm).

Acquisition protocol

The aorta was first filled with an iodine solution (hexabrix) through one of the connecting tube, to make it opaque to X-ray. A Right Anterior Oblique (RAO) projection at 45° of the opacified artery was acquired, followed by a Left Anterior Oblique 45 (LAO) projection. The iodine medium was then pushed out by injecting water, and RAO and LAO reference projections were acquired. The RAO and LAO reference projections were logarithmically subtracted from the RAO and LAO opacified images respectively. Two orthogonal DA were consequently obtained. They are shown on Fig. 1.

The X-ray tube was kept positioned on the LAO 45 incidence and the aorta was kept filled with water. The ultrasonic tranducer was then introduced into the aorta via the intravascular catheter and a first IVUS image was acquired as well as an X-ray LAO projection. The catheter-mounted transducer was then step by step manually withdrawn from small distances (approximately 1 mm by step) and couples X-ray control projections/IVUS images were acquired for each new position of the transducer. Figure 2 shows two pairs of X-rays/IVUS images for two different positions of the catheter through the vessel.

Preprocessings

Small motions of the examined artery may have occurred during the acquisition phase due to the introduction and moving of the transducer. To correct this possible motion, a matching of the two DA and control X-rays is performed using a global registration method with the metallic rings as external landmarks (10).

The reconstruction has been limited to a small portion of the vessel representing about 20 mm. The region of interest was selected on each DA (Fig. 1) as well as the corresponding IVUS slices and control X-rays.

GEOMETRIC FUSION

Representation of the acquisitions

The different data are then described into a unique reference frame (o, x, y, z) corresponding to the reference of the vessel to be reconstructed. It has been chosen such that the DA images correspond to the projections of the vessel on planes (xoy) and (xoz), respectively (Fig. 3a). To relate the IVUS images to the reference frame, an intermediate frame (O, X, Y, Z) corresponding to the transducer reference is introduced defined by a translation vector (x_t, y_t, z_t) and three rotation angles $(\theta, \varphi, \omega)$ (Fig. 3b).

Equations relating polar contour points (r, α) of an IVUS image to their Cartesian ones (x, y, z) in the reference frame are subsequently derived from this geometric modeling. Detailed calculations have been reported in a previous paper (10).

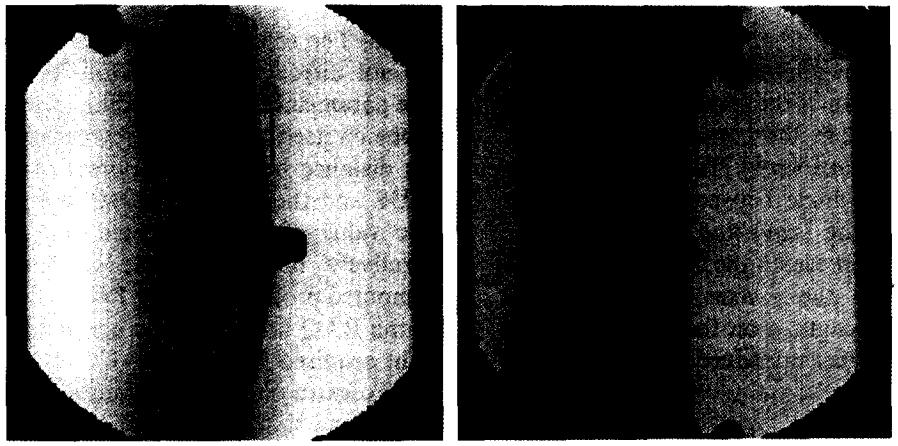

Fig. 1. Orthogonal Digital Angiographies of the aorta fixed on its support. (a) Left Oblique 45° projection, (b) Right Oblique 45° projection. The boxed areas indicate the region where the reconstruction is performed.

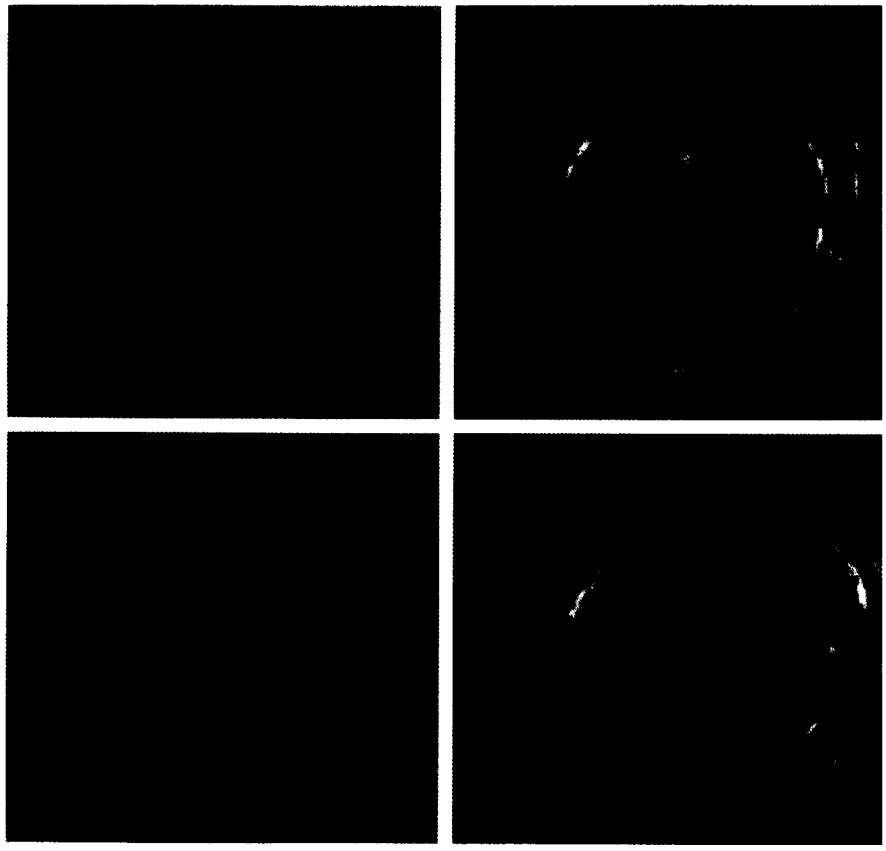

Fig. 2. On the left are two control radiographies showing two different positions of the catheter. On the right are the two corresponding IVUS slices.

The geometric description of ultrasonic slices into the reference frame thus consists of determining six parameters: x_t, y_t, z_t, θ, φ and ω.

Extraction of the geometrical parameters from the X-ray and US images

(a) The translation parameters x_t and y_t correspond to the tip position of the transducer and can be directly determined from the control X-rays which are acquired in the plane (xoy). The parameter θ is directly given by the angle between the transducer projection on the plane (xoy) and the x axis. The parameter φ which represents the angular deviation of the transducer to the z axis is given by the apparent transducer length ρ on the image which is related to the known real transducer length L by the relationship:

$$\varphi = \arcsin(\rho/L). \quad (1)$$

The transducer projected length, orientation and position are precisely estimated for each control X-ray by enlarging the catheter tip region (Fig. 4a) and enhancing the transducer by a simple thresholding (the transducer is more radio-opaque than the catheter and the non-opacified water-filled vessel) (Fig. 4b).

(b) The rotation ω and translation z_t parameters are not directly accessible from the control X-rays. The parameter ω corresponding to the rotation of the probe on itself is computed by iteratively minimizing, the distance between the points extracted from the IVUS and the contour extracted from the left DA. The value of z_t is estimated in the same way by iteratively minimizing the distance between the computed projection of the IVUS contours according to the RAO angle and the contours detected on the right acquired DA.

To extract the IVUS transversal contours which correspond to the change of acoustic impedance due to the interface lumen/intimal wall, a robust-to-noise fuzzy classification technique is performed followed by mathematical morphology operators in order to

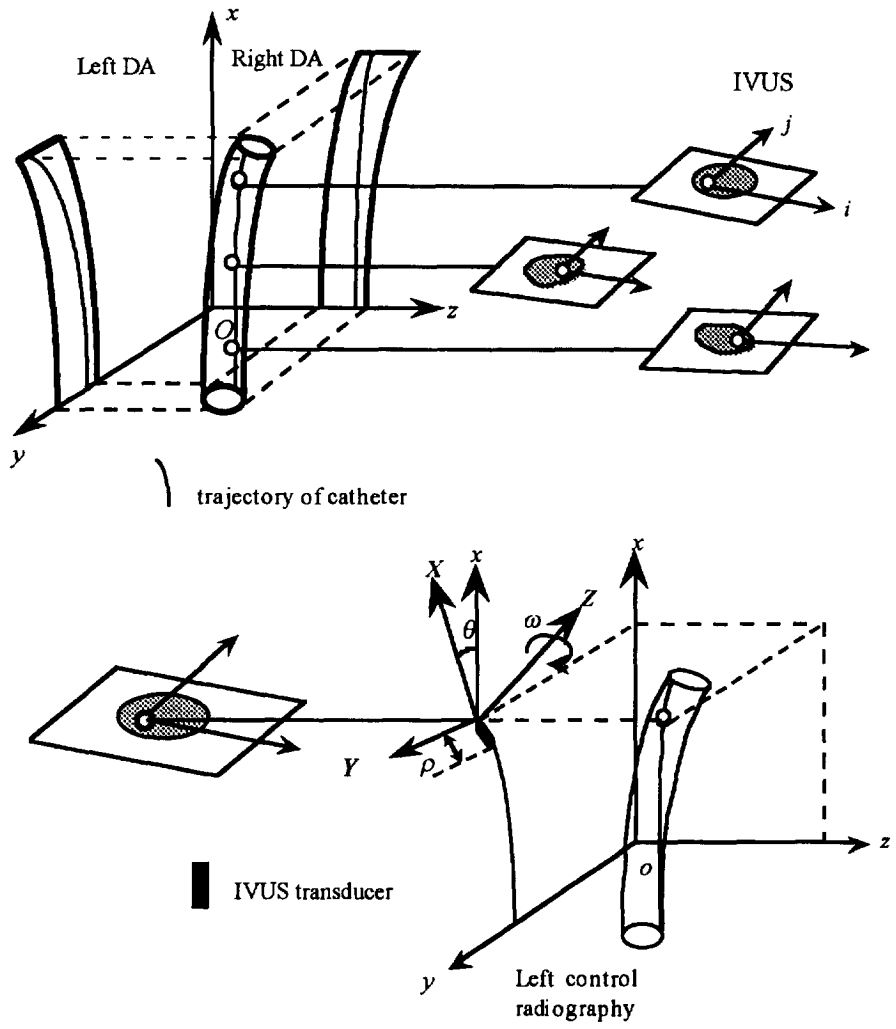

Fig. 3. (a) On the left, reference frame (o, x, y, z) given by the two DA planes, and on the right, IVUS reference frame (i, j). (b) IVUS transducer reference (O, X, Y, Z) related to (o, x, y, z) for a given position of the catheter.

select the vessel inner-wall and close contours (10). Figure 4c shows the resulting contours for the first IVUS of Fig. 2.

Vessel longitudinal contours on DA images are obtained by a dynamic tracking algorithm integrating parallelism constraints between vessel lumen centerline and borders. This method has been reported in (11).

Figure 5a shows the registered ultrasonic transversal contours superimposed on the DA segments of interest.

A linear interpolation of the IVUS contours registered in the reference frame is then performed in order to obtain a regularly-sampled 3D surface with the same resolution as angiographies. By assigning a value 1 to voxels inside the 3D surface and 0 outside, a binary 3D initial volume V_{IVUS} is obtained.

This 3D surface constitutes an approximate geometric reconstruction from IVUS and control radiographs, and already represents a significant improvement compared to slice-stacking techniques which do not take into account the degrees of freedom of the catheter.

PROBABILISTIC FUSION AND RECONSTRUCTION

Thus far, the X-ray densitometric information related to the vessel thickness, which is given by the gray levels of the DA images, has not been taken into account. The densitometric information of the vessel lumen only is obtained by extracting the region between the detected contours, subtracting the contribution of the background and normalizing

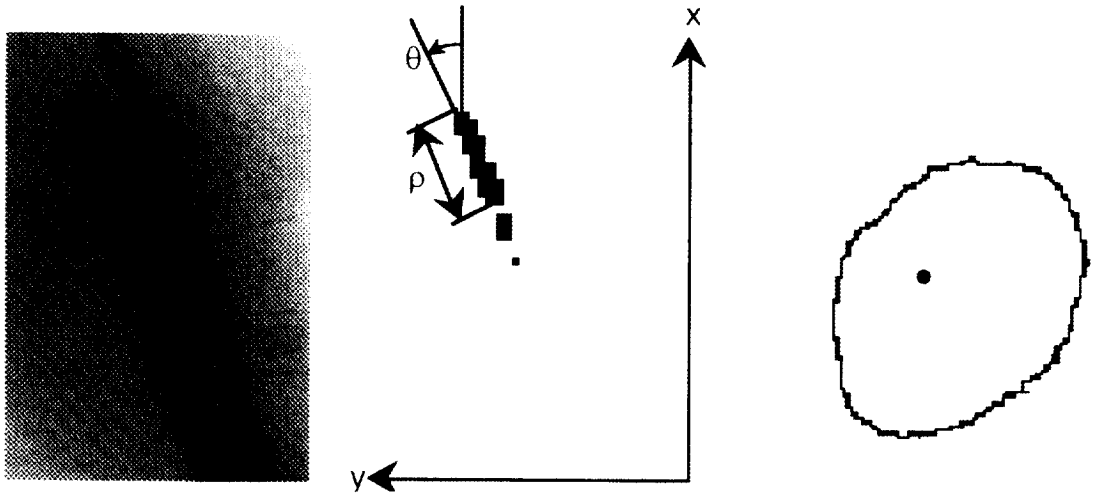

Fig. 4. (a) Enlargment of the edge region of the transducer on the control radiography, (b) extracted transducer after thresholding and (c) extracted contour of the IVUS slice.

the two DA views (11). The resulting densitometric images are represented on Fig. 5a.

The X-ray densitometric information and the 3D binary registered volume V_{IVUS}, which are available in the same reference frame, are then combined.

For that purpose, we start from an initial 3D configuration and we successively optimize each slice x by iteratively deforming it in order to fit the acquired data, i.e. the corresponding binary cross-section S_x of V_{IVUS} (Fig. 5c) and the two density

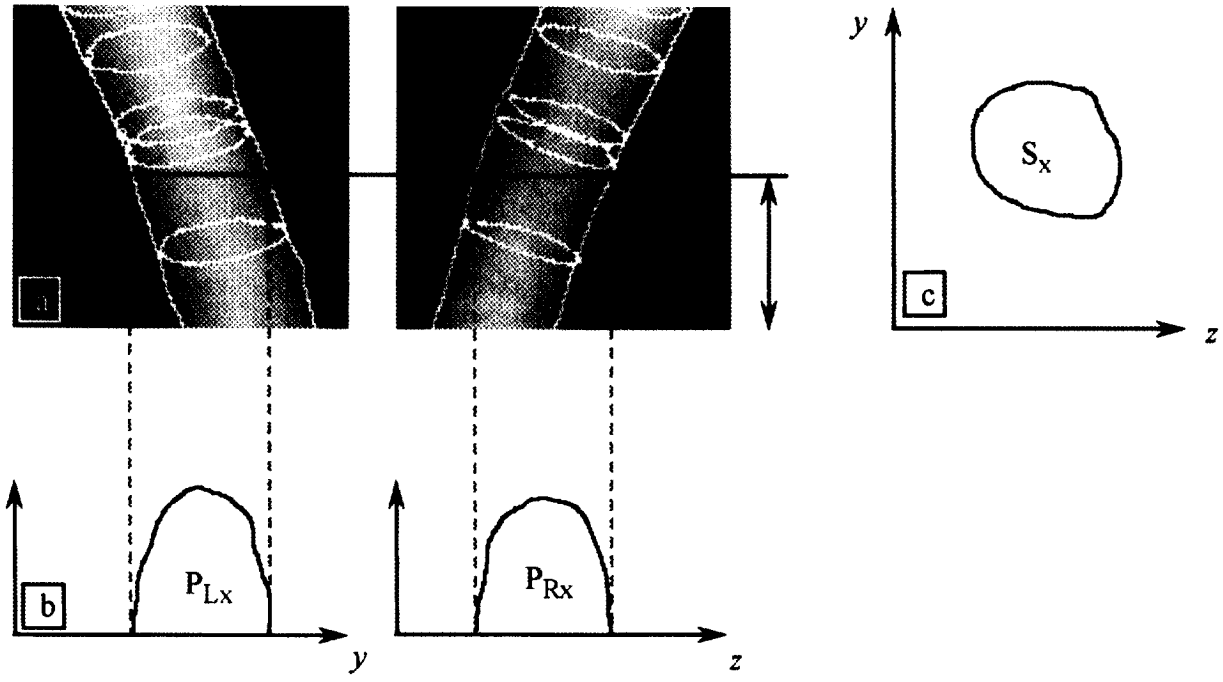

Fig. 5. Illustration of the geometric fusion. (a) DA and IVUS contours superimposed on the Left and Right DA segments of interest obtained after background subtraction. (b) Density profiles of the Left and Right DA segments at level x. (c) A binary cross-section of the registered and interpolated echographic volume, sliced at level x.

profiles P_{Rx} and P_{Lx} extracted from the two acquired DA at the corresponding cross-sectional level x (Fig. 5b). Considering the 3D reconstruction as a multiple 2D reconstruction problem by dividing the 3D volume to reconstruct into a stack of parallel cross-sections is a commonly used approach which permits to reduce the 3D problem complexity (12–14).

Simulated annealing

In a previous work (1), we developed a 3D reconstruction method from two projections based on a Markovian modeling of the vessel associated with an optimization algorithm based on Simulated Annealing (SA). The method of SA is well suitable for such optimization problems where a desired global extremum is hidden among many local extrema, which is the case here in the indeterminate problem of reconstruction from limited data. To make use of this algorithm, one must define an objective function E (analog of energy) whose minimization is the goal of the procedure. SA makes analogy with thermodynamics, where an heated-up-until-melting metal is imposed slow cooling, allowing ample time for redistribution of the atoms as they lose mobility. In this manner, lower energy states of the thermodynamic system are reached (15).

In 1953, Metropolis first incorporated these kinds of principles into numerical calculations. Offered a succession of options, a simulated system, in state k, is assumed to change its configuration from energy E_k to E_{k+1} with probability:

$$\begin{Bmatrix} p = 1 & \text{if } E_{k+1} < E_k \\ p = \exp[-E_{k+1} - E_k)/\kappa T] & \text{if } E_{k+1} > E_k \end{Bmatrix}$$

where T is a control parameter called temperature and k is a constant which relates the temperature to the energy (Boltzmann constant).

The probability p expresses the idea that a system in thermal equilibrium at temperature T has its energy probabilistically distributed among all different energy states.

The algorithm starts with a high temperature where most changes are accepted. The temperature T is then progressively decreased so that the changes corresponding to a positive variation of energy ($\Delta E = E_{k+1} > E_k$) become more and more rare. However, even at low temperature, there is a corresponding chance for the system to get out of a local energy minimum in favor of finding a better, more global one.

The general scheme of always taking a downhill step while sometimes authorizing an uphill step is known as the Metropolis algorithm.

Annealing schedule

Our reconstruction–fusion problem is handled as a problem in SA. The SA algorithm iteratively generates a sequence of neighboring configurations that form a Markov chain (16). Starting from an initial configuration, generator of random changes (or options) in the configuration are proposed.

To make the convergence to the optimal more efficient in our specific case of image restoration from projections, some adaptations of the SA algorithm have been performed.

A configuration in our case is an $N_1 \times N_2$ pixel matrix corresponding to a vessel cross-section whose pixel values are 0 or 1. The initial configuration is obtained by a least-square fitting of an oriented ellipse on each vessel cross-section using the density profiles P_R and P_L provided by the two DA. This initial configuration guides the reconstruction towards an homogeneous and compact shape which is anatomically more realistic than a multi-pieces shape. Moreover, since healthy or regular concentric stenosed vessels have elliptic cross-sectional projections, the initial solution is already close to the optimal one in those simple cases and the optimization step is fast. Pixels inside the ellipse are set to 1, pixels outside are set to 0.

Options are then proposed which consist of randomly choosing a pixel candidate for transition and replacing its value by its complementary binary value. To prevent changes of pixels in already homogenous area, candidate pixels for transition are pixels that belong to a contour or isolated pixels, consistent with the fact that atheroma deposits on the intimal wall and never occurs in the middle of the lumen. Series of changes along all actual candidate pixels are performed at constant temperature levels which are called a cycle.

Moves are achieved according to the Metropolis probability criterion defined above (Equation (2)), which requires the definition of an energy function.

Energy function

The energy is defined in the frame of Markov Random Fields (17) as a function of potential functions which express the cost relative to the DA and IVUS data consistency. In fact, the combination of only the two types of data can be for some areas incomplete or redundant. To solve these indeterminate cases, an anatomical *a priori* knowledge of homogeneity on the vascular structure is added. The energy model thus achieves a compromise between data consistency and regularization.

The data consistency consists of a two-term cost function. The first term is relative to the quadratic

difference between acquired projections and computed projections of the currently reconstructed configuration. The second term is relative to the quadratic Euclidean distance between the contours of V_{IVUS} and those of the current configuration. The regularization element reflects the contour energy of the reconstructed configuration and it imposes an increasing cost as the cross-section perimeter over the endovascular surface increases.

The energy for a reconstructed cross-section x is expressed as follow:

$$E_x = \lambda_1 \left[\frac{1}{N_L} \sum_y \left(P_{Lx}(y) - \hat{P}_{Lx}(y) \right)^2 + \frac{1}{N_R} \sum_z \left(P_{Rx}(z) - \hat{P}_{Rx}(z) \right)^2 \right]$$

$$+\lambda_2 \left[\frac{1}{N_E} \sum_{y,z} D(y,z) \left[S_x(y,z) - \hat{S}_x(y,z) \right]^2 \right]$$

$$+\lambda_3 \left[\frac{1}{N_E} \sum_{y,z} \sum_{k,l} \left[nc - \delta\left(\hat{S}_x(y,z), \hat{S}_x(k,l) \right) \right] \right]$$

where:

N_L and N_R are the DA normalization coefficients

N_E is the IVUS normalization coefficient ($N_E = N_L * N_R$)

P_{Lx} and P_{Rx} are the acquired density profiles at level x

$\hat{P}_{Lx}$ and $\hat{P}_{Rx}$ are the computed profiles of the current reconstructed configuration

S_x is a binary 2D pixel matrix obtained by slicing V_{IVUS} at level x

$\hat{S}_x$ is the matrix of the current estimated configuration

D is a cost function relative to the Euclidean distance between a pixel (y,z) in the reconstructed cross-section and the nearest contour point of the ultrasonic registered slice S_x. It is computed with a Chamfer operator, which imposes an increasing cost as pixels are further away from the contour (18).

δ is the Kronecker symbol defined as

$$\begin{cases} \delta(a,b) = 1 & \text{if } a = b \\ \delta(a,b) = 0 & \text{if } a \neq b \end{cases}$$

nc is the number of connexities ($nc = 8$ in the present application) and (k,l) are neighbors of (y, z) in eight connexities ($k = \{y - 1, y + 1\}, l = \{z - 1, z + 1\}$).

λ_1, λ_2 and λ_3 are the weighting coefficients of the energy function.

SA parameters

The optimal parameters of the SA schedule, which yield the best visual results while keeping reasonable convergence times have been determined.

- The initial temperature T_0 is estimated as a function of the difference between the initial elliptic configuration and the acquired data, since the closer the initial configuration to the optimal one, the lower must be the initial temperature required to converge. This permits rapid convergence of configurations already consistent with data.
- The temperature decrease law is: $T_{k+1} = 0.95\ T_k$, where k is the cycle number.
- The cycle length depends on the vessel perimeter. It typically varies between 3 and 5 times the perimeter of the initial elliptic configuration.
- The algorithm stops when the number of agreed transitions during a few successive cycles (typically 5) remains low (smaller than a quarter of the cross-section size).

To accelerate the probability determination which requires an exponential operation, the variation of energy ($\Delta E = E_{k+1} - E_k$) associated to a pixel transition is directly estimated instead of calculating the energy E_{k+1} for each option and subtracting it from the previous energy E_k (1). Probabilities corresponding to all possible energy variations are pre-calculated as a function of the temperature.

The optimal weightings of the energy function (λ_1, λ_2 and λ_3) have been heuristically adjusted by trying different combinations and estimating the one providing the best reconstruction. They are illustrated in the next section.

RESULTS AND DISCUSSION

Figures 6, 7 and 8 illustrate the reconstruction obtained with three different weightings of the energy elements. The left and right projections of the reconstructed segments are shown on the top left side of each figure. The difference images obtained by subtraction of the acquired projections after background elimination from the computed projections of the reconstructed segment are shown on the top right side of each figure. On the bottom of each figure four regularly-spaced transversal slices of the reconstructed segment are represented in order to visualize the intravascular shape and check its anatomical realistic aspect.

Figure 6 shows the reconstruction obtained using only data consistency with the IVUS interpolated volume V_{IVUS} ($\lambda_1 = 0$, $\lambda_2 = 1$ and $\lambda_3 = 0$). This reconstruction actually corresponds to the interpo-

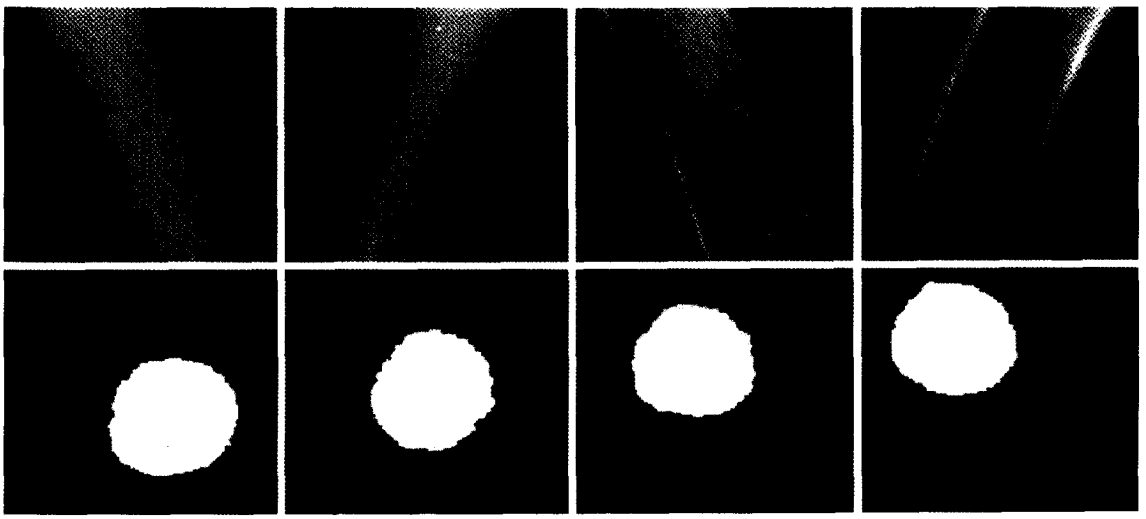

Fig. 6. Reconstruction obtained using only IVUS data consistency ($\lambda_1 = 0$, $\lambda_2 = 1$, $\lambda_3 = 1$). On the top, (a) and (b) LAO and RAO projections of the reconstructed structure. (c) and (d) Difference images obtained by subtracting the original segmented left and right projections from the reconstructed ones. On the bottom, four regularly-spaced cross-sectional images along the reconstructed vessel.

lated volume previously obtained in the geometrical fusion step (section 3). Difference between acquired angiographies and reconstructed projections are located on the borders of the projection images, which indicate an underestimation of the vessel geometry (Fig. 6c and d). These differences are in part due to imprecisions in the estimation of the geometrical fusion parameters.

Figure 7 shows the reconstruction from only data consistency with the angiographic data and regularization ($\lambda_1 = 1$, $\lambda_2 = 0$ and $\lambda_3 = 2$). It corresponds to the reconstruction obtained from two DA projections, reported in the previous paper (1). This reconstruction provides a small difference with the acquired projections which is normal, since only data consistency with DA and regularization have been taken into account. However, when looking closer at the slices of the reconstructed volume (bottom of the figure), the 2D morphology of the lumen looks different from the global shape of the corresponding IVUS registered images (Fig. 6e–g) which is not anatomically likely.

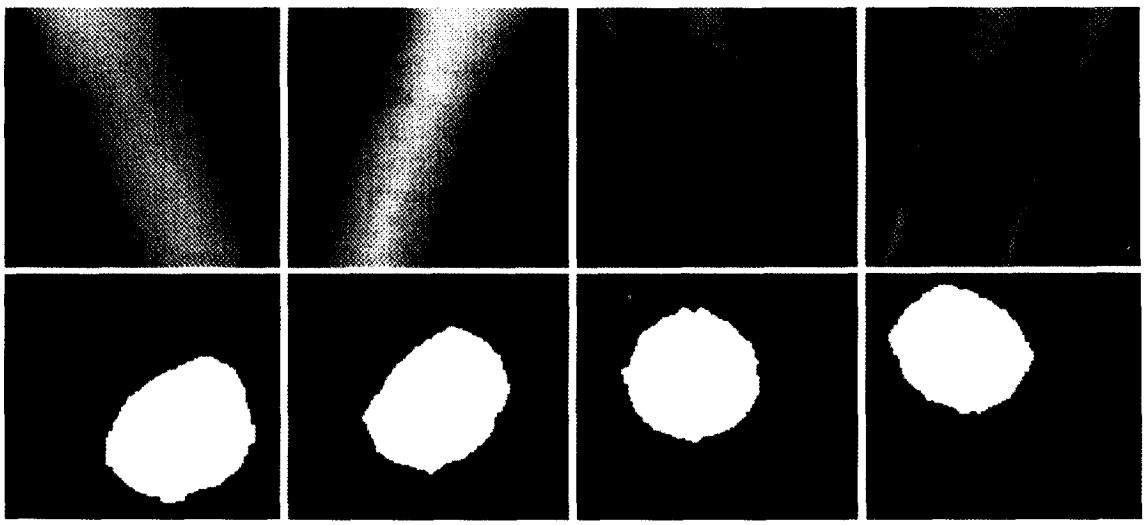

Fig. 7. Reconstruction obtained using only DA data consistency and regularization ($\lambda_1 = 1$, $\lambda_2 = 0$ and $\lambda_3 = 2$).

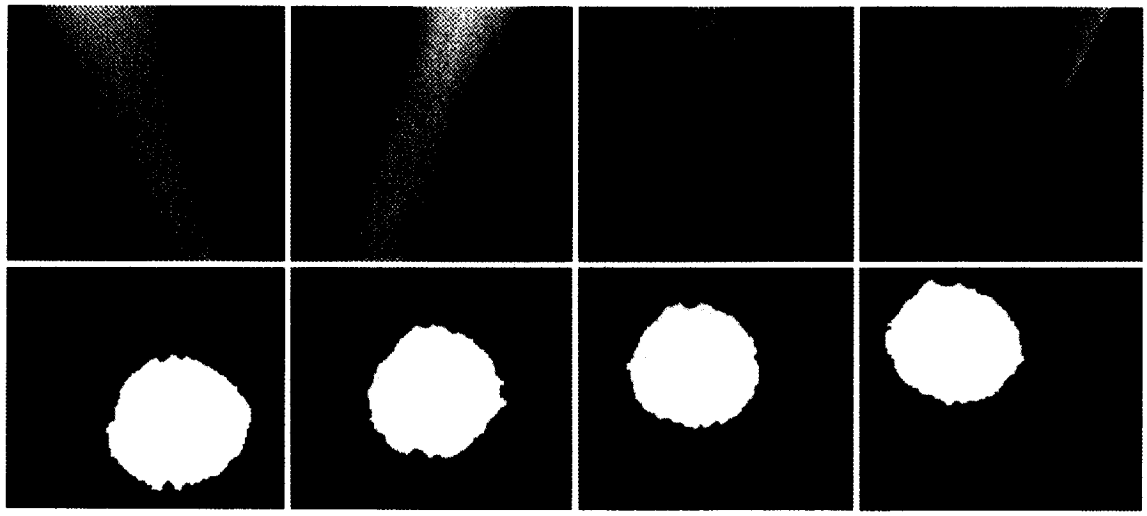

Fig. 8. Reconstruction obtained using IVUS and DA data consistency as well as regularization ($\lambda_1 = 0.5$, $\lambda_2 = 1$ and $\lambda_3 = 1$).

Figure 8 shows the reconstruction obtained with a good compromise between the three energy components ($\lambda_1 = 0.5$, $\lambda_2 = 1$ and $\lambda_3 = 1$). The difference images obtained when the two modalities are taken into account indicates both a good consistency between acquired DA projections and computed ones (top of Fig. 8), and similarity between the shapes of the reconstructed cross-sections and the IVUS ones (bottom of Fig. 8). This reconstruction is more accurate since the high resolution of IVUS slices is integrated while the reprojected structure remains consistent with DA data.

The results obtained from this probabilistic fusion have been compared to those obtained from a fuzzy approach which consisted of taking into account imprecision on the geometric fusion parameters in a process associating fuzzy modeling and mathematical morphology for the reconstruction (10). Both methods show good and similar results which reinforce the reliability of the fusion approach to 3D reconstruct vessels.

CONCLUSION

A possible methodological approach has been proposed for the 3D reconstruction of the vascular lumen only, based on a geometric then probabilistic fusion between X-ray and IVUS data. The fusion proposed here is a real combination of data which takes advantage of their complementariness to obtain a more complete knowledge of the 3D vessel morphology as well as of their redundancy to reduce imprecision and uncertainty on acquired data.

The approach consists of sequential process. From the purely geometric fusion of X-ray and IVUS data, approximate orientations and positions of IVUS images are described in the reference frame attached to DA, which by interpolation allow the determination of an approximate volume. Each vessel cross-section is then independently reconstructed in the reference of projections. From an initial elliptic solution, the optimal reconstruction is obtained by minimizing, through a SA process, the energy characterizing the Markov model of the cross-section, which represents a compromise between acquired data consistency as well as regularization. The combination of data takes place in the data consistency term, which contains a quadratic difference cost between acquired DA projections and those computed from the reconstructed structure ones as well as a distance-to-contour weighted quadratic difference cost between acquired IVUS images and computed cross-sections.

Preliminary results of the reconstruction obtained by fusion of *in vitro* acquired data shows an improved accuracy compared to results obtained from only one modality. Indeed, information on the longitudinal vessel geometry provided by DA are completed by detailed information on the 2D shape of vessel cross-sections provided by IVUS through this combination process.

This paper is a part of an ongoing study about 3D morphologic description and characterization of the vessel lumen and wall. Tissue characterization elements on possible atheromateous plaques provided by the IVUS textural data will be further

introduced in the fusion process to establish more thoroughly a knowledge on the vessel lesion. This will permit one to guide therapeutic procedures and improve their long-term effectiveness which is currently compromised by unsatisfactory outcomes such as restenosis.

REFERENCES

1. Pellot, C.; Herment, A.; Sigelle, M.; Horain, P.; Maitre, H.; Peronneau, P. A 3D reconstruction of vascular structures from two X-ray angiograms using an adapted Simulated Annealing algorithm. IEEE Trans. Med. Imag. 13:48–60; 1994.
2. Glagov, S.; Weisenberg, E.; Zarins, C.K.; Stankunavicius, R.; Kolettis, G.J. Compensatory enlargement of human atherosclerotic coronary arteries. N. Engl. J. Med. 316:1371–1375; 1987.
3. Beatt, K.J.; Serruys, P.W. Restenosis following coronary angioplasty. Int. J. Cardiac Imag. 5:155–162; 1990.
4. St. Goar, F.G.; Pinto, F.J.; Alderman, E.L.; Fitzgerald, P.J.; Stadius, M.L.; Popp, R.L. Intravascular ultrasound imaging of angiographically normal coronary arteries: an *in vivo* comparison with quantitative angiography. JACC 18:952–958; 1991.
5. Macovski, S.; Karouny, E.; Battaglia, S.; Bayet, G.; Diebold, B.; Guermonprez, J.L. Echographie endocoronaire: actualites et perspectives. Sang Thrombose Vaisseaux 5:691–696; 1993.
6. Kitney, R.J.; Moura, L.; Straughan, K. 3D visualization of arterial structures using ultrasound and voxel modeling. Int. J. Cardiac Imag. 4:135–143; 1989.
7. Klein, H.M.; Gunther, R.W.; Verlande, M.; Schneider, W.; Vorwerk, D.; Kelch, J., Hamm, M. 3D-surface reconstruction of intravascular ultrasound images using personal computer hardware and a motorized catheter control. Cardiovasc. Intervent. Radiol. 15:97–101; 1992.
8. Maurincomme, E.; Magnin, I.; Finet, G.; Goutte, R. Methodology for three-dimensional reconstruction of intravascular ultrasound images. SPIE Medical Imaging IV: Image Capture. Formatting and Display 1653:26–34; 1992.
9. Hoff, H.; Korbijn, A.; Smit, T.H.; Kinkhaumer, J.F.F.; Bom, N. Image artifacts in mechanically driven ultrasound catheters. Int. J. Cardiac Imag. 4:195–199; 1989.
10. Sureda, F.; Bloch, I.; Pellot, C.; Herment, A. Reconstruction 3D de vaisseaux sanguins par fusion de données a partir d'images angiographiques et échographiques. Traitement du Signal 13:48–60; 1994.
11. Pellot, C.; Herment, A.; Sigelle, M.; Horain, P.; Peronneau, P. Segmentation, modelisation and reconstruction of arterial bifurcations in Digital Angiography. Med. Biol. Engng Comput. 30:576–583; 1992.
12. Kenet R.O.; Herrold E.M.; Jearney G.J.; Wong K.K.; Hill J.P.; Borer J.S. 3D quantitative assessment of coronary luminal morphology using biplane digital angiography. Proc. IEEE Comput. Cardiology, Jerusalem; 1989: 13–17.
13. Van tran, L.; Bahn, R.C.; Sklansky, J. Reconstructing the cross-sections of coronary arteries from biplane angiograms. IEEE Trans. Med. Imag. 11:517–529; 1992.
14. Van den Broek, J.G.M.; Slump, C.H.; Storm, C.J.; van Benthem, A.C.; Buis, B. Three-dimensional densitometric reconstruction and visualization of stenosed coronary artery segments. Comput. Med. Imag. Graphics 19:207–217; 1995.
15. Press, W. Numerical recipes in C: the art of programming. Cambridge: Cambridge University Press; 1994: 454–455.
16. Geman, S.; Markov Graffigne, C. Random fields image models and their applications to computer vision. In: Gleason, A.M., ed. Proc. Int. Cong. Math. Providence Am. Math. Soc.; 1987.
17. Sigelle, M.; Ronfard, R. Potts models and image labeling by random Markov fields. Traitement du Signal 9:449–458; 1992.
18. Borgefors, G. Distance transformations in arbitrary dimensions. Comput. Vision Graphics Image Process. 27:321–345; 1984.

About the Author—CLAIRE PELLOT received the PhD degree in Biophysics from the University of Paris XI, France, in 1991. Since 1993, she has been a Chargée de Recherches at the Institut National de la Santé et de la Recherche Médicale (INSERM). She is currently affiliated with the Unité INSERM 66. Since 1996, she has been a visiting researcher in the Department of Radiology at the University of California, Davis. Her interests include data fusion of 3D morphologic and functional images from different modalities (Digital Angiography, Intravascular Ultrasound, Duplex Echography, MRA).

About the Author—ISABELLE BLOCH receveived the Degree of Ingénieur Civil des Mines in 1986, and the PhD Degree from the Ecole Nationale Superieure des Telecommunications (ENST), Paris in 1990. Since 1991, she has been with the Image Department at ENST, Paris, as assistant professor, and associate professor since 1993. Her interests include 3D object processing, fuzzy sets, 3D and fuzzy mathematical morphology, data fusion, decision theory, medical and satellite imagery, discrete geometry and 3D algorithmic.

About the Author—ALAIN HERMENT received an Engineering Degree in Electronics in 1973, and a PhD Degree in Physics from the University of Paris, France in 1984. He worked first as an engineer at the Centre National de la Recherche Scientifique (CNRS). Since 1977, he has been Directeur de Recherches at INSERM. His interests include signal and image processing for cardiovascular applications, mainly in the fields of echography, ultrasonic and MR velocimetry, Ultrafast CT and Digital Angiography.

About the author—FRANCISCO SUREDA received the Degree of Ingénieur of ETSE Telecom, Barcelona in 1992, and the Masters Degree from ENST Paris. He is currently working at General Electric, Paris. His interests include 2D and 3D medical image processing, with main applications in classification and 3D reconstruction.